Tellus (2005), 57B, 116–123
Printed in UK. All rights reserved

TELLUS

Test of a northwards-decreasing ^{222}Rn source term by comparison of modelled and observed atmospheric ^{222}Rn concentrations

By LYNETTE B. ROBERTSON[1,*], DAVID S. STEVENSON[1] and FRANZ CONEN[2], [1]*School of GeoSciences, University of Edinburgh, Mayfield Road, Edinburgh EH9 3JU, UK;* [2]*Environmental Geosciences, University of Basel, Bernoullistrasse 30, 4056 Basel, Switzerland*

(Manuscript received 26 March 2004; in final form 25 October 2004)

ABSTRACT

Model-predicted atmospheric concentrations of ^{222}Rn based on two different ^{222}Rn source terms have been compared with observations in the lower troposphere. One simulation used a globally uniform ^{222}Rn source term from ice-free land surfaces of 1 atom cm^{-2} s^{-1}; the other assumed a northwards-decreasing source term (linear decrease from 1 atom cm^{-2} s^{-1} at 30°N to 0.2 atom cm^{-2} s^{-1} at 70°N). Zero emissions were assigned to oceans. The northwards-decreasing source term improved predictions at four out of six stations north of 50°N, reducing the mean prediction/observation ratio from 2.8 to 0.87. In the latitudinal band between 30°N and 50°N, the northwards-decreasing source term resulted in systematic under-prediction of atmospheric ^{222}Rn, whereas the uniform source term provided predictions close to observations. Predictions based on the northwards-decreasing source term were significantly ($p < 0.01$) better than those based on the uniform source term for an averaged vertical ^{222}Rn profile around 44°N, but were not for one around 38°N. The results indicate that a northwards-decreasing source term could be a more realistic representation of actual ^{222}Rn emissions than a uniform 1 atom cm^{-2} s^{-1} source term. However, the decrease in ^{222}Rn source strength with increasing latitude might not begin at 30°N but somewhat further north. This hypothesis should be investigated through model-independent means.

1. Introduction

The radioactive noble gas ^{222}Rn (half-life = 3.82 d) is frequently used in the evaluation and intercomparison of atmospheric transport models (Brost and Chatfield, 1989; Feichter and Crutzen 1990; Genthon and Armengaud, 1995; Lin et al., 1996; Jacob et al., 1997; Stevenson et al., 1998; Dentener et al., 1999; Rasch et al., 2000; Taguchi et al., 2002; Chevillard et al., 2002; Collins et al., 2002). In this context, a uniform ^{222}Rn source term of ~1 atom cm^{-2} s^{-1} from all ice-free land surfaces is generally assumed. This value is between the global mean estimates of 0.72 atom cm^{-2} s^{-1} (Lambert et al., 1982) and 1.2 atom cm^{-2} s^{-1} (Turekian et al., 1977), and is thought to be accurate to within 25% globally and a factor of 2 regionally (Jacob et al., 1997 and references therein). In an attempt improve model predictions of atmospheric ^{222}Rn concentrations, some workers have modified this uniform ^{222}Rn flux distribution so as to take into account some of the variability in ^{222}Rn emissions. For example, Lee and Feichter (1995) assumed a reduced source strength of 0.005 atom cm^{-2} s^{-1} between 60 and 70°N, to account for apparent snow cover and soil freezing effects, and found that this improved model predictions of ^{210}Pb deposition rates. This source distribution was also used in the 1993 World Climate Research Program (WCRP) sponsored intercomparison of global atmospheric transport models (Jacob et al., 1997), and a similar modification (0.5 atom cm^{-2} s^{-1} between 60 and 70°N) was made in the 1995 WCRP workshop (Rasch et al., 2000). Other modifications of the ^{222}Rn source term which have been used include: accounting for a small oceanic flux (Heimann et al., 1990; Taguchi et al., 2002); taking into account variations in emissions due to soil texture (Dentener et al., 1999; Chevillard et al., 2002) and snow cover (Dentener et al., 1999); and increased emissions from Southeast Asia (Dentener et al., 1999; Taguchi et al., 2002). Some have also tried to improve ^{222}Rn predictions by taking into account temporal changes in ^{222}Rn flux (Jacob and Prather, 1990; Genthon and Armengaud, 1995; Lin et al., 1996). However, where any effects of these spatial and temporal modifications on predicted concentrations has been found, they have generally not been quantified.

Recently, a more far-reaching modification in the global ^{222}Rn flux term has been proposed by Conen and Robertson (2002).

*Corresponding author.
e-mail: lynette.robertson@ed.ac.uk

It is based on an empirical relationship between ^{222}Rn emissions and latitude which has been derived from published indirect ^{222}Rn flux measurements and estimates calculated from ^{210}Pb fluxes. With this distribution of emissions, the ^{222}Rn flux is 1 atom cm^{-2}s^{-1} between 60°S and 30°N, and from thereon decreases linearly to 0.2 atom cm^{-2}s^{-1} at 70°N. ^{222}Rn emissions are expected to decrease with increasing latitude in the Northern Hemisphere as a result of the increasing proportion of wetlands and organic soils (Stillwell-Soller et al., 1995; Conen and Robertson, 2002). Only ^{222}Rn produced in aerated surface layers of the soil is likely to escape to the atmosphere before its decay. Regional gradients in soil ^{226}Ra content caused by geochemical weathering patterns may also contribute to this trend, as appears to be the case in China where concentrations of ^{222}Rn precursors decrease from south to north (Xu et al., 1993; Sun et al., 2004). South of 60°S and north of 70°N, ^{222}Rn emissions are assumed to be zero. However, small fluxes (0.077 atom cm^{-2} s^{-1}) have been reported at 62°S during the brief Antarctic summer (Evangelista and Pereira, 2002). In this paper, we present the results of a study to find if this new source term improves predictions of ^{222}Rn compared with use of the uniform ^{222}Rn source term of 1 atom cm^{-2} s^{-1} between 60°S and 70°N. The observational data used were long-term average ^{222}Rn concentrations for 23 ground-based stations and two averaged vertical profiles. The model used was STOCHEM-Ed (Stevenson et al., 2003), a new version of the UK Met Office global chemistry-transport-model (CTM), first described in Collins et al. (1997).

2. Observations, model and simulations

2.1. Surface observations

The data used for surface comparisons were published monthly mean ^{222}Rn concentrations available for 22 sites located at different latitudes, and data for the Cape Grim baseline air pollution station (W. Zahorowski, personal communication). The locations of these stations are shown in Fig. 1a, and details of each site are summarized in Table 1. Station locations range in latitude from 68°N (Pallas, Finland) to the South Pole, with 13 stations north of 30°N and 10 stations south of 30°N. Long-term means of surface ^{222}Rn concentrations were calculated from reported monthly means, except for Mauna Loa and Bermuda, where published values were monthly medians. For Pallas and New York City, where ^{222}Rn concentrations have been published for more than

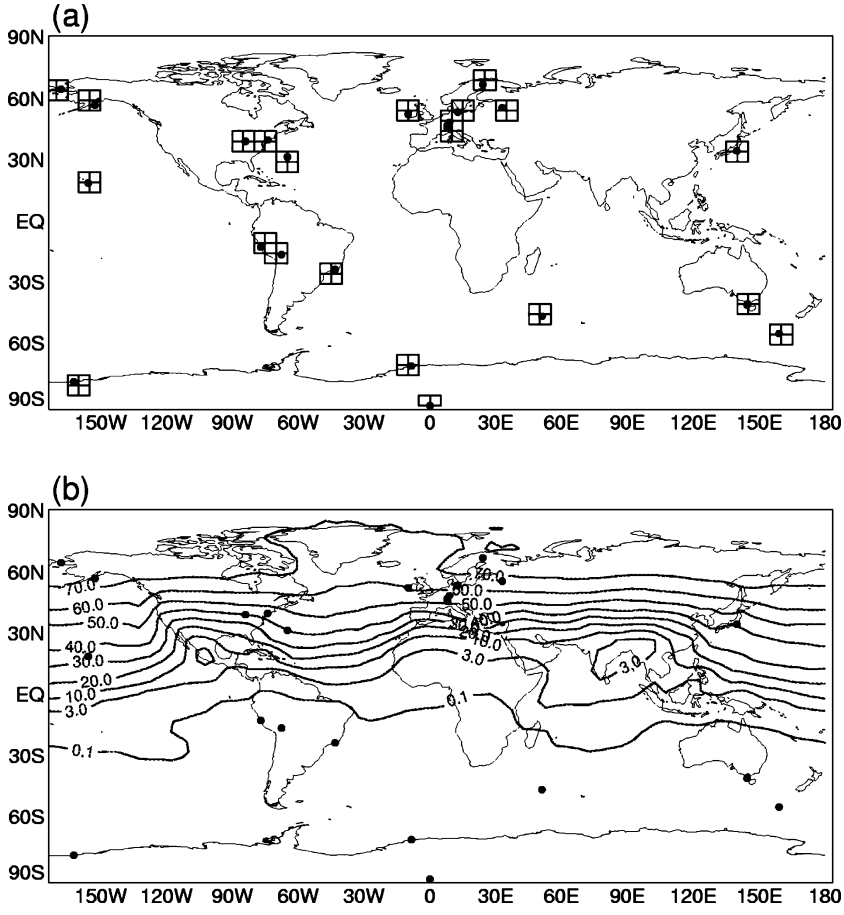

Fig 1. (a) Location of stations where atmospheric ^{222}Rn has been measured for more than 2 months and model grid cells used in the prediction of ^{222}Rn concentrations at these stations. (b) The relative change (%) in ^{222}Rn concentrations when changing to the northwards-decreasing emissions distribution.

Table 1. Location of stations where measurements of atmospheric ^{222}Rn concentrations have been performed for durations of more than 2 months

Latitude	Longitude	Station	Type	Period of observation	Data source
68.0°N	24.1°E	Pallas, Finland	Polar	7 yr	Hatakka et al. (2003)
65.6°N	168.0°W	Wales, Alaska	Coastal	7 yr	Lockhart (1962)
57.8°N	152.5°W	Kodiak, Alaska	Marine	11 yr	Lockhart (1962)
56.5°N	32.9°E	Fyodorowskoye, Russia	Continental	Jul, Oct, 1 yr	Chevillard et al. (2002)
54.4°N	12.7°E	Zingst, Germany	Coastal	Mar, Jul, Oct, 1 yr	Chevillard et al. (2002)
53.3°N	9.9°W	Mace Head, Ireland	Coastal	Jun–Aug, 2 yr	Biraud et al. (2002)
49.4°N	8.9°E	Heidelberg, Germany	Continental	Mar, Jul, Oct, 1 yr	Chevillard et al. (2002)
47.9°N	7.9°E	Schauinsland, Germany	Continental	4.5 yr	Schmidt et al. (1996)
46.6°N	8.0°E	Jungfraujoch, Switzerland	Continental	1 yr	Gäggeler et al. (1995)
40.7°N	73.9°W	New York City	Coastal	2 yr	Fisenne and Keller (1996)
40.0°N	84.0°W	Cincinnati, Ohio	Continental	4 yr	Gold et al. (1964)[a]
35.3°N	139.7°E	Yokosuka, Japan	Coastal	4.5 yr	Lockhart (1959)
32.3°N	64.9°W	Tudor Hill, Bermuda	Marine	4 yr	EML (2003)
19.5°N	155.6°W	Mauna Loa, Hawaii	Marine	3 yr	Hutter et al. (1995)
12.0°S	77.0°W	Lima, Peru	Coastal	1 yr	Lockhart (1960)
15.7°S	67.6°W	Chacaltaya, Bolivia	Continental	1.5 yr	Lockhart (1960)
23.0°S	43.2°W	Rio de Janeiro, Brazil	coastal	2 yr	Lockhart (1960)
40.4°S	144.4°E	Cape Grim, Tasmania	Coastal	15 yr	W. Zahorowski (pers. com.)
46.0°S	51.0°E	Crozet Island	Marine	27 yr	Lambert et al. (1995)[a]
54.5°S	159.0°E	Macquarie Island	Marine	Apr, Nov, 2 yr	Whittlestone and Zahorowski (1998)
70.6°S	8.4°W	G. v. Neumayer, Antarctica	Polar	6 yr	Wyputta (1997)
78.2°S	162.2°W	Little America V, Antarctica	Polar	2.5 yr	Lockhart (1960)
90.0°S		South Pole	Polar	1 yr	Lockhart (1960)

[a]In Jacob et al. (1997).

one height, we chose the greatest available height as the most representative of the concentrations in the lowest layer in our model. For Pallas this was Sammaltunturi station, which is on a hillside 565 m above sea level (asl) and around 200 m above the surrounding area, and for New York City this was 260 m above street level. By averaging over the longest timescale available, much of the temporal variation in ^{222}Rn concentrations is eliminated (Robé et al., 1992). Thus, comparisons with predictions become less subject to the ability of the model to faithfully reproduce temporal variations in ^{222}Rn concentrations, and a larger proportion of any discrepancy between prediction and observations becomes attributable to the differences between the actual and assumed ^{222}Rn source terms or systematic deficiencies in the model. One measure of the discrepancy between prediction and observation we have used is the average of prediction/observation ratios; the other is the root-mean-square error of prediction relative to observation.

2.2. *Vertical profile observations*

The vertical profile data used were those published in Kritz et al. (1998) and Zaucker et al. (1996). These data are the most recent, reliable and detailed ^{222}Rn profile data available. The data in Kritz et al. (1998) were collected in the vicinity of Moffet Field, California, USA (∼38 °N, 122°W). Measurements were made during the period from 3 June to 16 August 1994 and consisted of 11 flights up to 11.5 km altitude. The data in Zaucker et al. (1996) were collected over Nova Scotia, New Brunswick, and the western North Atlantic Ocean (∼44°N, 64°W), with flights originating from Halifax. These measurements were made between the 16 and 31 August 1993 as part of the North Atlantic Regional Experiment (NARE) campaign, and consisted of nine flights up to 5500 m. For each data set, an average ^{222}Rn profile was compiled from the separate flights by averaging measured values over 1000 m intervals, and 2000 m intervals for greater altitudes. No interpolation was made. The measurements were compared with the model layers corresponding to the same height intervals.

2.3. *Model*

STOCHEM-Ed is a new version of the UK Met Office 3-D Lagrangian CTM STOCHEM (e.g. Collins et al., 1997; Collins et al., 2000, 2002), developed at the University of Edinburgh. STOCHEM-Ed is closely coupled to the Unified Model (UM) general circulation model (GCM) (Johns et al., 1997), from which it is receiving meteorological fields every 3 h. Earlier versions of STOCHEM have taken part in a number of intercomparisons regarding transport and chemistry, including the 1995 WRCP workshop (Rasch et al., 2000). In all of these studies the model was typically found to perform well within the

range of other current models. Thus, we would expect the results of this study to also be valid for other global atmospheric models, although this should be tested.

STOCHEM-Ed uses a Lagrangian transport scheme, dividing the atmosphere into 50 000 air parcels of equal mass. These parcels are advected by winds from the GCM with a fourth-order Runge–Kutta algorithm, using linear horizontal interpolation and cubic vertical interpolation, and adding a small random walk component to simulate turbulent diffusive mixing. The parcels maintain an approximately even global distribution with time. Convective mixing is implemented by fully mixing a fraction of the parcels beneath a convective cloud top. The precipitation rate and fractional cloud cover determine the amount mixed (Stevenson et al., 1998). Interparcel mixing occurs between parcels occupying the same grid box after each 1 h advection step. Turbulent mixing in the boundary layer is achieved by randomly reassigning the vertical coordinates of air parcels over the depth of the layer. The grid used for mixing is $5^\circ \times 5^\circ$, with 22 vertical hybrid (η) levels (six levels with $\Delta\eta = 0.1$ between $\eta = 1.0$ and $\eta = 0.4$, 15 levels with $\Delta\eta = 0.025$ between $\eta = 0.4$ and $\eta = 0.025$, and a top level between $\eta = 0.025$ and $\eta = 0.0003$). Hybrid coordinates are explained further in Collins et al. (1997), but can be considered as approximately equal to pressure divided by surface pressure. The vertical resolution of the surface boundary layer in STOCHEM-Ed is quite coarse, with the lowest six levels being approximately 100 hPa thick ($\sim$1 km). The boundary layer is therefore typically represented by only one or two levels. The top level is in the stratosphere, well above the highest level of interest for ^{222}Rn (approximately tropopause levels). The driving GCM has a more highly resolved boundary layer, which is represented by six different levels. Surface trace gas emissions are added to air parcels within the boundary layer above their sources. Gridded emission distributions with a horizontal resolution of $5^\circ \times 5^\circ$ are used. When several air parcels occupy the boundary layer for the grid square, emissions are divided equally between them. If no air parcels are present, for example when the boundary layer is very shallow, emissions are stored until the next time step, ensuring mass conservation. A more detailed description of STOCHEM-Ed can be found in Stevenson et al., 2003.

2.4. Simulations

For each ^{222}Rn source term one 15-month simulation was carried out, the first 3 months of which were discarded as spin-up time. The meteorological driver (UM) was configured as an atmosphere-only GCM, with a resolution of 3.75° longitude by 2.5° latitude and with 58 vertical levels between the surface and 0.1 hPa. Recent climatologies of sea-surface temperatures and stratospheric ozone were used to drive the GCM. The modelled values of ^{222}Rn for each station are linearly interpolated from the four surrounding grid boxes, where the values for a grid box are taken to be representative of its central latitude and longitude. These grid boxes are illustrated in Fig. 1a. For all stations except Mauna Loa (3400 m asl) and Jungfraujoch (3580 m asl) the ^{222}Rn concentrations used in the comparison were for the lowest model layer. For Mauna Loa this was the second layer. At Jungfraujoch, strong diurnal variations in ^{222}Rn with maxima during late afternoon in summer, and the absence of variations in winter, indicate the influence of the convective boundary layer in summer and exposure to the free troposphere in winter (Gäggeler et al., 1995). Thus, for Jungfraujoch we used model layer 2 (centred 1200 m above the local ground surface) for June to September, and model layer 3 (centred 2000 m above the local ground surface) the rest of the year.

3. Results and discussion

The assumption of a decreasing ^{222}Rn source strength north of 30°N only notably affected predicted ^{222}Rn concentrations in the Northern Hemisphere (Table 2), as we would expect given the mean atmospheric (or e-folding) lifetime of ^{222}Rn of 5.5 d. Differences in atmospheric ^{222}Rn concentrations between the two simulations were largest in the surface layer polewards of 40°N, with peak differences towards the centres of large land masses (Canada and Siberia). In relative terms, the northwards-decreasing source term resulted in a reduction of more than 70% in surface layer concentrations northwards of 60°N (Fig. 1b). This difference between the two simulations decreased steadily with decreasing latitude, and at 30°N was less than 10% over the continents and less than 30% over the centre of the oceans.

In this study, the approach taken to comparing predictions with observations is somewhat different from that of previous studies. For each site, predictions and observations have been averaged over the longest timescale available, without taking into account variations over shorter timescales (e.g. Dentener et al., 1999; Taguchi et al., 2002). In this way, the influence of random errors in the comparison, for both observations and predictions, has been reduced. We did not attempt to judge the quality of the measurements reported, assuming that instrumental bias is distributed randomly among the 23 stations and averages zero. Using the largest number of stations possible should then result in the smallest bias in the overall judgement. If the model is a perfect representation of reality and bias among the stations is distributed as assumed, we would expect prediction and observation to converge towards the same value with increasing averaging time and increasing number of stations included in the comparison. If this is not the case, systematic deficiencies of the model, the observations or both could be responsible. However, currently, the most important systematic uncertainty in matching predictions with observations seems to be uncertainties in ^{222}Rn emissions (Schery and Wasiolek, 1998; Chevillard et al., 2002); thus, the similarity of predicted and observed long-term averages at a large number of stations should be an indication of the accuracy of the ^{222}Rn source term employed.

Table 2. Observed and predicted long-term ^{222}Rn concentrations (in Bq m^{-3}) for two different ^{222}Rn source term assumptions

Latitude	Station	Observation	Prediction		Prediction/observation ratio	
			Uniform	Northwards-decreasing	Uniform	Northwards-decreasing
68.0°N	Pallas	1.22	1.54	0.43	1.26	0.36
65.6°N	Wales	0.74	0.98	0.25	1.33	0.33
57.8°N	Kodiak	0.36	1.94	0.51	5.32	1.39
56.5°N	Fyodorowskoye	1.45	4.62	1.44	3.19	1.00
54.4°N	Zingst	1.33	3.27	1.24	2.46	0.93
53.3°N	Mace Head	0.44	1.44	0.53	3.26	1.20
49.4°N	Heidelberg	4.13	3.31	1.45	0.80	0.35
47.9°N	Schauinsland	2.02	3.17	1.48	1.57	0.73
46.6°N	Jungfraujoch	0.58	0.81	0.42	1.40	0.73
40.7°N	New York City	3.40	3.25	1.78	0.96	0.52
40.0°N	Cincinnati	5.04	3.71	2.23	0.74	0.44
35.3°N	Yokosuka	2.06	2.12	0.97	1.03	0.47
32.3°N	Tudor Hill	0.46	0.59	0.36	1.29	0.78
19.5°N	Mauna Loa	0.18	0.11	0.07	0.59	0.40
12.0°S	Lima	1.15	1.94	1.94	1.69	1.69
15.7°S	Chacaltaya	1.44	2.64	2.64	1.84	1.84
23.0°S	Rio de Janeiro	1.52	1.28	1.28	0.85	0.85
40.4°S	Cape Grim	0.68	0.59	0.59	0.87	0.87
46.0°S	Crozet Island	0.04	0.07	0.07	1.60	1.60
54.5°S	Macquarie Island	0.05	0.05	0.05	0.94	0.94
70.6°S	Georg v. Neumayer	0.03	0.02	0.02	0.76	0.76
78.2°S	Little America V	0.10	0.01	0.01	0.09	0.09
90.0°S	South Pole	0.02	0.01	0.01	0.53	0.53

Table 3. Surface data mean prediction/observation ratios and root-mean-square error of prediction relative to observation (RMSE) for three areas of geographical coverage

Geographical coverage	No of stations	Mean prediction/observation ratio		RMSE	
		Uniform	Northwards-decreasing	Uniform	Northwards-decreasing
North of 50°N	6	2.80	0.87	2.27	0.42
30°N–50°N	7	1.11	0.58	0.31	0.45
South of 30°N	10	0.97	0.96	0.53	0.55
Global	23	1.49	0.82	1.22	0.49

Globally, the northwards-decreasing ^{222}Rn source term resulted in a mean prediction/observation ratio (0.82) closer to unity than the uniform source term assumption (1.49) (Table 3). Also, the root-mean-square error was smaller: 0.49 for the northwards-decreasing source term compared with 1.22 for the uniform source term assumption. However, when we take a more differentiated look we find that this improvement was mainly due to an improvement in prediction at stations north of 50°N, where predictions were improved at four out of six stations. For stations north of 50°N the uniform source term resulted in an almost three-fold (2.80) overestimation, whereas predictions based on the northwards decreasing source term were relatively close to unity (0.87). Yet, in the latitudinal band between 30°N and 50°N, predictions based on the uniform source term were closer to observations at four out of seven stations and mean prediction/observation ratios were much closer to unity (1.11) than for predictions based on the northwards decreasing source term (0.58). South of 30°N, little difference was found between the two sets of predictions. In both cases, mean prediction/observation ratios were close to unity (0.97; 0.96) and the root-mean-square error was slightly over 0.5. This last result gives some confidence in the model not being particularly biased

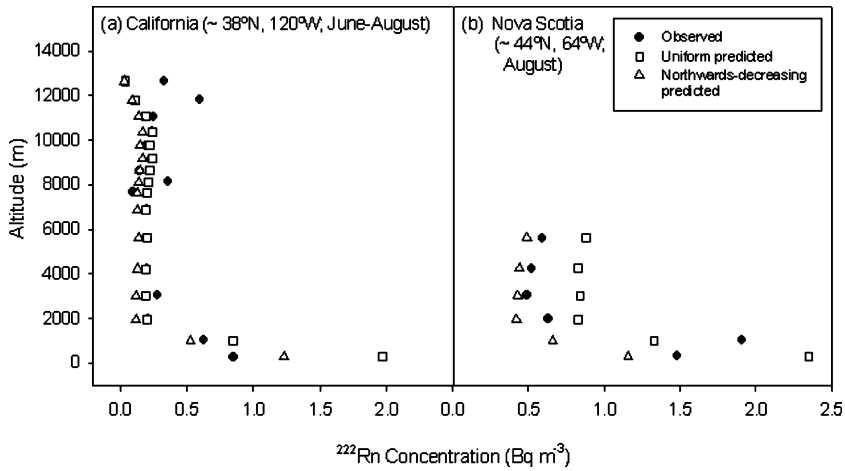

Fig 2. Observed and predicted ^{222}Rn concentrations for (a) the California region and (b) the Nova Scotia and North Atlantic Ocean region. Observed concentrations are the average from all flights made during the measurement campaign.

towards under- or overestimation. Thus, for our comparison of different ^{222}Rn source terms we can suppose that both the better results north of 50°N as well as the underestimate between 30°N and 50°N for the northwards-decreasing source term assumption are likely to be genuine.

Predicted and observed ^{222}Rn concentrations for the two vertical profiles are shown in Fig. 2. Mean ^{222}Rn concentrations were greater for the Nova Scotia/North Atlantic Ocean profile (Zaucker et al., 1996) than for the Californian profile (Kritz et al., 1998), despite the fact that air samples for the first profile were largely collected over the ocean. However, given the predominantly westerly winds at these latitudes, west coast locations are likely to be more strongly influenced by ^{222}Rn-poor maritime air, and east coast locations more strongly influenced by ^{222}Rn-rich continental air, and thus ^{222}Rn concentrations will tend to be greater on the east coast of the continent. The largest differences in absolute terms between the two sets of predicted concentrations occur in the surface layer, as we would expect. In relative terms, however, the decrease was as large or larger at higher levels. The differences are greater for the Nova Scotia profile than for the California profile because of the higher latitude of this region (Fig. 2). At 44°N (the latitude of the Nova Scotia profile) the northwards-decreasing source term assumes 28% less emission, but only 16% less at 38°N (the latitude of the Californian profile). Mean prediction/observation ratios and the root-mean-square error of prediction relative to observation for each profile are given in Table 4. For the Nova Scotia data there was substantial improvement in model predictions when changing to the northwards-decreasing ^{222}Rn source term, especially at heights above 2000 m. The mean prediction/observation ratio for all height intervals altered from 1.40 to 0.72, and the root-mean-square error of prediction relative to observation was reduced from 0.52 to 0.33. Changing to the northwards-decreasing ^{222}Rn source term shifted the mean prediction/observation ratio away from unity for the California profile, but predictions were improved for the lowest two height intervals. Similar results to this (improved prediction for the Nova Scotia profile but no improvement for the California profile) have been found by Gupta et al. (2004), in a study in which they compared the northwards-decreasing source term with the source term used in the 1993 WCRP workshop (Jacob et al., 1997). As for the results for the surface data, this observation suggests that the northwards-decrease in ^{222}Rn source strength begins somewhat north of 30°N.

4. Conclusions

The comparison of observed and predicted ^{222}Rn concentrations lends, in general, support to the assumption of a decrease in ^{222}Rn source strength with increasing latitude in the Northern Hemisphere. Empirical evidence based on indirect ^{222}Rn flux measurements and estimates derived from ^{210}Pb fluxes suggests

Table 4. Vertical profile mean prediction/observation ratios and root-mean-square errors of prediction relative to observation (RMSE)

		Mean prediction/observation ratio		RMSE	
Region	No of height intervals	Uniform	Northwards-decreasing	Uniform	Northwards-decreasing
Nova Scotia	6	1.40	0.72	0.52	0.33
California	16	1.04	0.69	0.55	0.46

that fluxes decrease northwards of 30°N. However, the validation of this suggestion through comparison of predicted and observed atmospheric ^{222}Rn concentrations yielded mixed results. While the northwards-decreasing source term substantially improved predictions north of 50°N compared with a uniform source term of 1 atom cm^{-2} s^{-1}, it also resulted in a systematic underprediction of ^{222}Rn concentrations in the latitudinal band between 30°N and 50°N, a region where predictions based on the uniform source term were closer to observations. Although this study does not provide a proof of one particular source term it indicates that the northwards-decreasing source term is a more realistic representation than the generally used uniform 1 atom cm^{-2} s^{-1} source term. It also suggests that this decrease begins somewhere between 30°N and 50°N, rather than at 30°N as indicated by the available flux measurements. Future investigations into ^{222}Rn fluxes should therefore concentrate on these latitudes. Whilst this study suggests a geographical region where further refinement might be necessary, appropriate investigation needs to be made by other means, otherwise the derived source term will not be model-independent and therefore cannot be used in future model validations. Guidance for further improvement of ^{222}Rn parametrization has recently been worked out in an expert meeting supported by the World Meteorological Organization/Global Atmosphere Watch (WMO/GAW, 2004). This includes, amongst others, the quest for quality controlled measurements of ^{222}Rn emissions along north–south transects in Europe and North America, and improved knowledge of global surface ^{226}Ra concentrations.

5. Acknowledgments

We are grateful to the Cape Grim baseline air pollution station and to Dr Wlodek Zahorowski of the Australian Nuclear Science and Technology Organisation for providing atmospheric ^{222}Rn data for Cape Grim. DS thanks the Environment Agency (P4-F02) and the Natural Environmental Research Council (NERC) for fellowship funding (NER/J/S/2000/00840). LR carried out this research whilst in receipt of a NERC PhD studentship.

References

Biraud, S., Ciais, P., Ramonet, M., Simmonds, P., Kazan, V. et al. 2002. Quantification of carbon dioxide, methane, nitrous oxide and chloroform emissions over Ireland from atmospheric observations at Mace Head. *Tellus* **54B**, 41–60.

Brost, R. A. and Chatfield, R. B. 1989. Transport of radon in a three-dimensional, subhemispheric model. *J. Geophys. Res.* **94**, 5095–5119.

Chevillard, A., Ciais, P., Karstens, U., Heimann, M., Schmidt, M. et al. 2002. Transport of ^{222}Rn using the regional model REMO: a detailed comparison with measurements over Europe. *Tellus* **54B**, 850–871.

Collins, W. J., Derwent, R. G., Johnson, C. E. and Stevenson, D. S. 2000. The impact of human activities upon the photochemical production and destruction of tropospheric ozone. *Q. J. R. Meteorol. Soc.* **126**, 1925–1952.

Collins, W. J., Derwent, R. G., Johnson, C. E. and Stevenson, D. S. 2002. A comparison of two schemes for the convective transport of chemical species in a Lagrangian global chemistry model. *Q. J. R. Meteorol. Soc.* **128**, 991–1009.

Collins, W. J., Stevenson, D. S., Johnson, C. E. and Derwent, R. G. 1997. Tropospheric ozone in a global-scale 3-D Lagrangian model and its response to NO_x emission controls. *J. Atmos. Chem.* **26**, 223–274.

Conen, F. and Robertson, L. B. 2002. Latitudinal distribution of radon-222 flux from continents. *Tellus* **54B**, 127–133.

Dentener, F., Feichter, J. and Jeuken, A. 1999. Simulation of the transport of ^{222}Rn using on-line and off-line global models at different horizontal resolutions: a detailed comparison with measurements. *Tellus* **51B**, 573–602.

EML (Environmental Measurements Laboratory), 2003. *Environmental Measurements Laboratory Atmospheric ^{222}Rn database*. United States Department of Energy Environmental Measurements Laboratory, New York (http://www.eml.doe.gov/databases/radon/index.cfm).

Evangelista, H. and Pereira, E. B. 2002. Radon flux at King George Island, Antarctic Peninsula. *J. Environ. Radioactiv.* **61**, 283–304.

Feichter, J. and Crutzen, P. J. 1990. Parameterization of vertical tracer transport due to deep cumulus convection in a global transport model and its evaluation with ^{222}Radon measurements. *Tellus* **42B**, 100–117.

Fisenne, I. M. and Keller, H. W. 1996. Continuous indoor and outdoor measurements of ^{222}Rn in New York City: city as a source. *Environ. Int.* **22**, S131–S138.

Gäggeler, H. W., Jost, D. T., Baltensperger, U. and Schwikowski, M. 1995. Radon and thoron decay product and ^{210}Pb measurements at Jungfraujoch, Switzerland. *Atmos. Environ.* **29**, 607–616.

Genthon, C. and Armengaud, A. 1995. Radon-222 as a comparative tracer of transport and mixing in two general circulation models of the atmosphere. *J. Geophys. Res. Atmos.* **100**, 2849–2866.

Gold, S., Barkhau, H., Shleien, W. and Kahn, B. 1964. Measurement of naturally occurring radionuclides in air. In: *The Natural Radiation Environment* (eds J. A. S. Adams and W. M. Lowder). University of Chicago Press, Chicago, IL, 369–382.

Gupta, M. L., Douglass, A. R., Kawa, S. R. and Pawson, S. 2004. Use of radon for evaluation of atmospheric transport models: sensitivity to emissions. *Tellus* **56B**, 404–412.

Hatakka, J., Aalto, T., Aaltonen, V., Aurela, M., Hakola, H. et al. 2003. Overview of the atmospheric research activities and results at Pallas GAW station. *Boreal Environ. Res.* **8**, 365–383.

Heimann, M., Monfray, P. and Polian, G. 1990. Modelling the long-range transport of ^{222}Rn to sub-Antarctic and Antarctic areas. *Tellus* **42B**, 83–99.

Hutter, A. R., Larsen, R. J., Maring, H. and Merrill, J. T. 1995. Radon-222 at Bermuda and Mauna Loa: local and distant sources. *J. Radioanal. Nucl. Chem. Articles* **193**, 309–318.

Jacob, D. J. and Prather, M. J. 1990. Radon-222 as a test of convective transport in a general circulation model. *Tellus* **42B**, 118–134.

Jacob, D. J., Prather, M. J., Rasch, P. J., Shia, R. L., Balkanski, Y. J. et al. 1997. Evaluation and intercomparison of global atmospheric transport models using Rn-222 and other short-lived tracers. *J. Geophys. Res.* **102**, 5953–5970.

Johns, T. C., Carnell, R. E., Crossley, J. F., Gregory, J. M., Mitchell, J. F. B. et al. 1997. The second Hadley Centre coupled ocean-atmosphere GCM: model description, spinup and validation. *Clim. Dyn.* **13**, 103–134.

Kritz, M. A., Rosner, S. W. and Stockwell, D. Z. 1998. Validation of an off-line three-dimensional chemical transport model using observed radon profiles 1. Observations. *J. Geophys. Res.* **103**, 8425–8432.

Lambert, G., Polian, G., Ardouin, B., Renault, J. and Balkanski, Y. 1995. *CFR database of ^{222}Rn, ^{220}Rn, and ^{210}Pb in the sub-Antarctic and Antarctic atmosphere*. Centre des Faibles Radioactivites, Gif-sur-Yvette, France.

Lambert, G., Polian, G., Sanak, J., Ardouin, B., Buisson, A. et al. 1982. Cycle of radon and its daughters: application to the study of troposphere-stratosphere exchanges [in French]. *Ann. Geophys.* **38**, 497–531.

Lee, H. N. and Feichter, J. 1995. An intercomparison of wet precipitation scavenging schemes and the emission rates of ^{222}Rn for the simulation of global transport and deposition of ^{210}Pb. *J. Geophys. Res.* **100**, 23 252–23 270.

Lin, X., Zaucker, F., Hsie, E. Y., Trainer, M. and McKeen, S. A. 1996. Radon-222 simulations as a test of a three-dimensional regional transport model. *J. Geophys. Res.* **101**, 29 165–29 177.

Lockhart, L. B. 1959. Atmospheric radioactivity levels at Yokosuka, Japan, 1654–1958. *J. Geophys. Res.* **64**, 1445–1449.

Lockhart, L. B. 1960. Atmospheric radioactivity in South America and Antarctica. *J. Geophys. Res.* **65**, 3999–4005.

Lockhart, L. B. 1962. Natural radioactive isotopes in the atmosphere at Kodiak and Wales, Alaska. *Tellus* **14**, 351–355.

Rasch, P. J., Feichter, J., Law, K., Mahowald, N., Penner, J. et al. 2000. A comparison of scavenging and deposition processes in global models: results from the WCRP Cambridge Workshop of 1995. *Tellus* **52B**, 1025–1056.

Robé, M. C., Rannou, A. and Le Bronec, J. 1992. Radon measurement in the environment in France. *Radiat. Prot. Dosim.* **45**, 455–457.

Schery, S. D. and Wasiolek, M. A. 1998. Modelling radon flux from the Earth's surface. In: *Radon and Thoron in the Human Environment, Proceedings of the 7th Tohwa University International Symposium* (eds A. Katase and M. Shimo). World Scientific Press, Singapore, 207–217.

Schmidt, M., Graul, R., Sartorius, H. and Levin, I. 1996. Carbon dioxide and methane in continental Europe: a climatology, and ^{222}Radon-based emission estimates. *Tellus* **42B**, 457–473.

Stevenson, D. S., Collins, W. J., Johnson, C. E. and Derwent, R. G. 1998. Intercomparison and evaluation of atmospheric transport in a Lagrangian model (STOCHEM), and an Eulerian model (UM), using ^{222}Rn as a short-lived tracer. *Q. J. R. Meteorol. Soc.* **124**, 2477–2491.

Stevenson, D. S., Johnson, C. E., Highwood, E. J., Gauci, V., Collins, W. J. et al. 2003. Atmospheric impact of the 1783–1784 Laki eruption: Part I Chemistry modelling. *Atmos. Chem. Phys.* **3**, 487–507.

Stillwell-Soller, L. M., Klinger, L. F., Pollard, D. and Thompson, S. L. 1995. *The Global Distribution of Wetlands*. NCAR Technical Note NCAR/TN-416+STR, National Center for Atmospheric Research, Boulder, CO.

Sun, K., Guo, Q. and Zhuo, W. 2004. Feasibility for mapping radon exhalation rate from soil in China. *J. Nucl. Sci. Technol.* **41**, 86–90.

Taguchi, S., Iida, T. and Moriizumi, J. 2002. Evaluation of the atmospheric transport model NIRE-CTM-96 by using measured radon-222 concentrations. *Tellus* **54B**, 250–268.

Turekian, K. K., Nozaki, Y. and Benninger, L. K. 1977. Geochemistry of atmospheric radon and radon products. *Annu. Rev. Earth Planet. Sci.* **5**, 227–255.

Whittlestone, S. and Zahorowski, W. 1998. Baseline radon detectors for shipboard use: development and deployment in the first aerosol characterisation experiment (ACE 1). *J. Geophys. Res.* **103**, 16 743–16 751.

WMO/GAW, 2004. *1st International Expert Meeting on Sources and Measurements of Natural Radionuclides Applied to Climate and Air Quality Studies, Gif-sur-Yvette, France, 3–5 June 2003*. WMO TD No 1201 (http://www.wmo.ch/web/arep/reports/gaw155.pdf).

Wyputta, U. 1997. On the transport of trace elements into Antarctica using measurements at the Georg-von-Neumayer station. *Tellus* **49**, 93–111.

Xu, N., Wei, F. S., Ten, E. J. and Chen, L. Q. 1993. Evaluation of indigenous concentrations of uranium and thorium in soils of China. *Commun. Soil Sci. Plant Anal.* **24**, 1795–1803.

Zaucker, F., Daum, P. H., Wetterauer, U., Berkowitz, C., Kromer, B. et al. 1996. Atmospheric ^{222}Rn measurements during the 1993 NARE intensive. *J. Geophys. Res.* **101**, 29149–29164.